Modifications of Microvascular EC Surface Modulate Phototoxicity of a Porphycene anti-ICAM-1 Immunoconjugate; Therapeutic Implications

Citation: Rosas, Elisabet, Pablo Santoma, Miquel Duran-Frigola, Bryan Hernandez, Maria C. Llinas, Ruben Ruiz-Gonzalez, Santi Nonell, David Sanchez-Garcia, Elazer R. Edelman, and Mercedes Balcells. "Modifications of Microvascular EC Surface Modulate Phototoxicity of a Porphycene Anti-ICAM-1 Immunoconjugate; Therapeutic Implications." Langmuir 29, no. 31 (August 6, 2013): 9734–9743.

As Published: http://dx.doi.org/10.1021/la401067d

Publisher: American Chemical Society (ACS)

Persistent URL: http://hdl.handle.net/1721.1/92822

Version: Author's final manuscript: final author's manuscript post peer review, without publisher's formatting or copy editing

Published in final edited form as:
Langmuir. 2013 August 6; 29(31): . doi:10.1021/la401067d.

Modifications of microvascular EC surface modulate phototoxicity of a porphycene anti-ICAM-1 immunoconjugate; therapeutic implications

Elisabet Rosàs[†,‡], **Pablo Santomá**[†,‡], **Miquel Duran-Frigola**[†,‡], **Bryan Hernandez**[†,‡], **Maria C. Llinàs**[‡], **Rubén Ruiz-González**[‡], **Santi Nonell**[‡], **David Sánchez-García**[‡], **Elazer R. Edelman**[§], and **Mercedes Balcells**[†,‡,*]

[†]Massachusetts Institute of Technology, Institute for Medical Engineering Sciences, 77 Massachusetts Avenue, Cambridge, MA 02139

[‡]IQS School of Engineering, Univ Ramon Llull, Via Augusta 390, Barcelona 08017, Spain

[§]Cardiovascular Division, Brigham and Women's Hospital and Harvard Medical School, 75 Francis Street, Boston, MA 02115

Abstract

Inflammation and shear stress can upregulate expression of cellular adhesion molecules in endothelial cells (EC). The modified EC surface becomes a mediating interface between the circulating blood elements and the endothelium, and grants opportunity for immunotherapy. In photodynamic therapy (PDT), immunotargeting might overcome the lack of selectivity of currently used sensitizers. In this study, we hypothesized that differential ICAM-1 expression modulates the effects of a drug targeted to surface ICAM-1. A novel porphycene-anti-ICAM-1 conjugate was synthesized and applied to treat endothelial cells from macro and microvasculature. Results show that the conjugate induces phototoxicity in inflamed, but not in healthy, microvascular EC. Conversely, macrovascular EC exhibited phototoxicity regardless of their state. These findings have two major implications; the relevance of ICAM-1 as a modulator of drug effects in microvasculature, and the potential of the porphycene bioconjugate as a promising novel PDT agent.

Introduction

Inflammation and shear stress are powerful regulators of endothelial surface receptor expression (1-5). Receptor upregulation modifies the surface of endothelial cells (EC), creating a uniquely active interface between the intimal layer of the vessel wall and the circulating blood in the lumen (6). This biological interface becomes a critical mediator of cell-cell interactions and transport processes (4,7), providing an opportunity for receptor-specific therapies. Endothelial cell immuno-targeting has already reached successes in diverse fields such as cardiovascular, pulmonary, metabolic and oncologic disease (8-14). Intracellular adhesion molecule-1 (ICAM-1 or CD54) has been suggested to be the most suitable surface receptor for endothelial targeting (13,15). ICAM-1 is readily accessible and mainly exposed by ECs to the lumen of blood vessels, is upregulated by pathological factors, and has been implicated in the pathogenesis of a wide range of diseases (15-17). The

[*]To whom correspondence and proofs should be addressed. Massachusetts Institute of Technology, Institute for Medical Engineering and Science, 77 Massachusetts Avenue, building E25, room 438, Cambridge, MA 02139. merche@mit.edu, Tel.: (617) 324 0054, FAX: (617) 253 2514.

Supporting Information Available: Characterization (NMR and IR spectra) of the bioconjugation intermediate species.

recycling mechanism of ICAM-1 discovered by Muro *et al.* also renders this cellular adhesion molecule (CAM) a potential vehicle for sustained drug delivery (18).

In photodynamic therapy (PDT), immunotargeting might overcome lack of sensitizer selectivity, which constitutes one of the major drawbacks of the current therapy (19,20). PDT is a non-invasive treatment that utilizes photosensitizers to cause controlled cellular damage. Photodynamic sensitizers harness photons to generate, in the presence of molecular oxygen, a burst of reactive oxygen species (ROS), often singlet oxygen (21). ROS induce cell death in the neighborhood of the photosensitizer by reacting with a large variety of cell components, such as unsaturated fatty acids, proteins, and nucleic acids (21). In an attempt to enhance selectivity and achieve faster clearance from the blood stream, several studies have conjugated photosensitizers to monoclonal antibodies and antibody fragments (19,20,22). A highly effective method for sensitizer bioconjugation is based on the isothiocyanate (NCS)-porphyrin chemistry (19,22,23).

Combining PDT with immunotargeting of EC may provide alternative treatment options for cancer and various other disease processes where EC play a major role in the formation of neovasculature (24). Pathologic angiogenesis is indeed a key symptom of many diseases and can lead to severe, fatal complications (25-28). Targeting of microvascular EC in neovessels has already led to successful treatments such as regression of tumoral angiogenesis in cancer, or inhibition of choroidal neovascularization in macular degeneration (29,30). It remains unknown, however, whether inflammation- and shear stress-induced modifications of microvascular endothelial cell surface could modulate the phototoxic effects of an immunoconjugated PDT drug. Thus, in this study, we first investigated how cytokine and shear stress stimulation modifies ICAM-1 surface expression and anti-ICAM-1 uptake in macrovascular and microvascular EC. We then synthesized a novel porphycene-anti-ICAM-1 conjugate and tested the ability of the conjugate to discriminate between surface changes in EC resulting from altered ICAM-1 expression.

Materials and Methods

Cell Culture

Human coronary artery endothelial cells (HCAEC) and human dermal microvascular endothelial cells (HmVEC) (Promocell, Heidelberg, Germany) were cultured in EBM-2 basal medium (Promocell) supplemented with 5% fetal bovine serum, 1% penicillin-streptomycin, and the EGM-2 Supplement Pack (Promocell) containing 5ng/mL epidermal growth factor, 10ng/mL basic fibroblast growth factor, 20ng/mL insulin-like growth factor (R3 IGF-1), 0.5ng/mL vascular endothelial growth factor, 1μg/mL ascorbic acid, 22.5μg/mL heparin, and 1μg/mL hydrocortisone. Cells were used in passages 4 to 6, fed every 48h and cultured in a humidified incubator at 37°C and 5% CO_2.

In vitro flow model

HCAEC and HmVEC were seeded at a density of 1×10^6 cells/mL in a parallel plate flow chamber manufactured by IBIDI (μSlide I0.8 Luer, Ibiditreat, IBIDI, Munich, Germany). After allowing cells to adhere to the bottom slide overnight, flow chambers were imaged using a bright field inverted microscope (Nikon Diaphot) to ensure confluency, and subsequently connected to steady flow. Average shear stress levels applied were 18dyn/cm^2 and 8dyn/cm^2, for coronary and microvascular-like flow, respectively. Cells were exposed to flow for 12h in the presence of 3ng/mL TNF-α using a perfusion bioreactor as described in previous work (31). Controls without TNF- α and without flow were carried out in parallel.

Microscopic examinations

All steps were done at room temperature (RT) unless otherwise specified. Cells were fixed with 4% paraformaldehyde in PBS for 20min. After two 5min washes with PBS, samples were treated with 0.2M glycine in PBS for 10min. Then samples were washed twice for 5min with PBS and cells were permeabilized using 0.05% Triton X100 for 10min. After two consecutive 5min washes with PBS and blocking with 5% goat serum in PBS-BSA (PBS, 1% bovine serum albumin), cells were labelled overnight at 4°C with mouse monoclonal anti-VCAM-1 and anti- ICAM-1 (Santa Cruz Biotechnology), diluted 1:50 in PBS-BSA. Cells were rinsed twice with PBSBSA for 5min and stained with goat anti-mouse Alexa Fluor 647 or goat anti-mouse Alexa Fluor 488 secondary antibodies (1:100 in PBS-BSA, Invitrogen,) and DAPI solution (1μg/mL in PBSBSA) for 1h and 30min at RT. Two 5min washes with PBS were performed to remove any unbound antibody before imaging using a fluorescent microscope (Nikon Ti-E Perfect Focus Inverted Microscope). Mean fluorescence of cells was quantified using ImageJ.

Western Blot Analysis

HCAEC and HmVEC were seeded in tissue culture plates and grown to confluency. When confluent, half of the plates were treated with EGM-2 media containing 3ng/mL TNF-α for 12h, while the other half were kept in EGM-2 media as untreated, healthy controls. Untreated controls and TNF-α stimulated cells were lysed using RIPA Buffer (Sigma), freshly supplemented with protease inhibitor cocktail (Sigma) for 30 min at 0°C. Lysates were diluted in Laemmli buffer (Sigma) and 10% β-mercaptoethanol and boiled for 5 min. Samples were loaded in 10% acrylamide gels (Invitrogen, Carlsbad, Calif). Gels were blotted with Invitrogen iBlot® gel transfer stacks and dry blotting system. Membranes were blocked with 5% powdered milk and incubated with monoclonal rabbit anti-ICAM-1 (Cell Signaling, 1:1000 dilution) and anti-tubulin (loading control, Santa Cruz, 1:650 dilution) overnight at 4 °C while shaking. Membranes were washed twice with PBS-T (PBS, 0.05% Tween20) and incubated with horseradish peroxidase-conjugated secondary antibodies (Santa Cruz Bitechnology; 1:2000 dilution) for 45 min. After two 10 min washes with PBS-T, Luminata TM Forte Western HRP Substrate (Millipore) was applied for 1 min (diluted with deionized water 1:5 for tubulin and 1:1 for ICAM-1) and luminescence was detected for 30s using a molecular imager (ChemiDoc TM XRS+, Bio-Rad). Resulting densitometry plots were analyzed with ImageJ and normalized to the tubulin signal.

Antibody uptake by live cells under flow

HCAEC and HmVEC were seeded in parallel plate flow chambers as described above. 12h after seeding, samples were treated with 3ng/mL TNF-α for 12h. Anti-ICAM-1 conjugated to Alexa Fluor 488 (Santa Cruz Biotechnologies) was dialysed for 9h in sterile PBS to remove sodium azide and diluted in EBM-2 basal media to a final concentration of 0.1μM. Cells were exposed to shear stresses of 0, 8 or 18dyn/cm^2 using a perfusion bioreactor. Perfusate consisted of EGM-2 media containing the FITC-ICAM-1 antibody. Cells were imaged after 20min to 24h of flow exposure using a fluorescent microscope.

Synthesis of 9-glutaramide-2,7,12,17-tetra-phenylporphycene (GlamTPPo) (Scheme 1, 1)

44 mg (0.1 mmol) of 9-(glutaric methylesteramide)-2,7,12,17-tetra-phenylporphycene were first dissolved in 28 mL of a 1:1 mixture of tetrahydrofuran (THF) and methanol, and further hydrolyzed at room temperature with the dropwise addition (time≈5min) of 9mL of a 2N aqueous solution of sodium hydroxide. The reaction was stirred for 45min, and then neutralized and precipitated under acidic conditions with the addition of 50mL of 5% acetic acid previously cooled in an ice bath. The flaky, bluish precipitate was extracted with THF/ethyl acetate (EtOAc) (3 × 25mL), washed with water twice (25mL), and dried under

vacuum. Compound **2** (Scheme 2) was obtained in the form of a dark blue-green powder. Yield: 27mg (η = 70%).

Synthesis of GlamTPPoEdaBOC (Scheme 1, 3)

GlamTPPo (29mg, $3.9 \cdot 10^{-5}$mol) and benzotriazol-1-yl-oxytripyrrolidinophosphonium hexafluorophosphate (PyBOP, 25mg, $4.8 \cdot 10^{-5}$mol) were suspended in 10mL of dichloromethane (DCM) at 0°C under nitrogen atmosphere. Then 0.04mL of of *N*,*N*-diisopropylethylamine (DIPEA) was added. A solution of 1-(tert-butoxycarbonyl)ethyldiamine (7mg, $4.3 \cdot 10^{-5}$mol) (Sigma Aldrich, St. Louis, MO, USA) in 10mL of DCM was added after complete dissolution of all solids in the mixture. The solution was stirred overnight and monitored by TLC (ethylacetate (EtOAc)/ dichloromethane (DCM) = 1:1). After completion of the reaction, the solvent was removed under vacuum. The crude product was purified by silica gel column chromatography (AcOEt:EtOH = 30:1) to give compound GlamTPPoEdaBOC.

Synthesis of GlamTPPoEdaNCS (Scheme 1, 4)

GlamTPPoEdaBOC (15mg, 0,017mmol) was dissolved in 5mL of DCM. After dissolution of all solids, 0.5mL (6.5mmol) of trifluoroacetic acid (TFA) were added. The mixture was stirred and monitored by TLC (AcOEt:MeOH = 20:1). After completion of the reaction (time≈30min), the solvent was washed twice with saturated sodium bicarbonate solution and solvent was removed under vacuum to give compound GlamTPPoEda. The crude compound was dissolved in 5mL of DCM with further addition of 1,1'-thiocarbonydil-2(1*H*)-pyridone (7mg, 0,03mmol). The reaction mixture was stirred and monitored by TLC (AcOEt:Cyclohexane = 80:20). After completion of the reaction (time≈2h), the solvent was washed twice with sodium bicarbonate solution (25mL), and removed under vacuum. The crude product was purified by silica gel column chromatography (AcOEt:Cyclohexane= 50:50) to give compound GlamTPPoEdaNCS.

NMR spectra

^{1}H and ^{13}C NMR spectra were collected on a Varian 400-MR (^{1}H at 400 MHz and ^{13}C at 100.6 MHz) spectrometer. All NMR data were obtained in $CDCl_3$ and DMSO-d_6. Chemical shifts are reported in parts per million (ppm, δ) and are referenced to the residual proton signal of the solvent. Coupling constants are reported in Hertz (Hz). Spectral splitting patterns are designated as s: singlet, d: doublet, t: triplet, q: quartet, m: complex multiplet (chemically non-equivalent H's), brs: broad signal. Infrared spectra were recorded in a Nicolet Magna 560 FTIR spectrophotometer. All MS were registered at the Unidad de Espectrometria de Masas (Universidad de Santiago de Compostela) using a Micromass Autospec spectrometer. Flash chromatography was performed using silica gel 60 A C.C 35-70μm. Solvents and reagents were reagent-grade and were used without further purification (Sigma Aldrich, St. Louis, MO, USA).

Anti-ICAM-1-porphycene conjugate synthesis and preparation

1mg of mouse anti-human anti-ICAM-1 (Santa Cruz Biotechnologies) was dissolved in carbonate/bicarbonate buffer (pH=9.2) to obtain 1mg/mL antibody solution. 0.134 mg GlamTPPoEdaNCS were first dissolved in 50 μL anhydrous dimethylsulfoxide (DMSO) and then added to the antibody under a nitrogen atmosphere while shaking for 2h at RT. The antibody-porphycene conjugate (Scheme 2, 6) was purified using a Sephadex G-25M column (GE Health Care) eluted with PBS. Absorbance spectra were obtained to characterize the conjugate. The conjugate concentration (mg/mL) was quantified using Lambert-Beer law ($\varepsilon_{percent}$ = 13 $(g/100\ ml)^{-1} \cdot cm^{-1}$) (32). Conjugate was also analyzed by sodium dodecyl sulphate-polyacrylamide gel electrophoresis (SDS-PAGE).

Dark Toxicity Assay

HCAEC and HmVEC were seeded in 96-well plates at a density of 10^4 cells/cm^2. At confluency, half of the cells were activated with EGM-2 media containing 3ng/mL TNF-α (Sigma Aldrich, St. Louis, MO, USA) overnight, while the other half (unstimulated controls) were kept in EGM-2 media without TNF-α. Both stimulated and unstimulated HmVEC and HCAEC were incubated in the dark with increasing concentrations of anti-ICAM-1-porphycene conjugate solution (0.001- 1.0μM) in basal EBM-2 media for 4h. Time of incubation (4h) was determined by antibody uptake experiment previously described. Cells were washed twice with basal media and the 3- [4,5-dimethylthiazol-2-yl]-2,5-diphenyltetrazolium bromide (MTT) assay was performed to determine cell viability. Briefly, cells were incubated with 50μL of MTT solution (0.05mg/mL MTT in basal EBM-2, Sigma-Aldrich, St. Louis, MO, USA). After 3h incubation, the solution was removed to stop the reaction, and cells were lysed with DMSO for 30min while shaking. Vigorous pipetting was applied to dissolve the blue formazan crystals produced by the mitochondria of live cells. Absorbance of cell lysates was read at 562nm. Viability (%) of cells was calculated with respect to additional unstimulated controls that had not been incubated with conjugate.

Phototoxicity Assay

HCAEC and HmVEC were seeded in 96-well plates at a density of 10^4 cells/cm^2. At confluency, half of the cells were activated with 3ng/mL TNF-α (Sigma Aldrich, St. Louis, MO, USA) in EGM- 2 media for 12h, while the other half served as unstimulated controls. Cells were incubated in the dark for 4h with increasing concentrations of anti-ICAM-porphycene conjugate solution (0.001-1.0μM), prepared by diluting the conjugate in basal EBM-2 media. After 2 washes with PBS (to eliminate unbound photosensitizer), EGM-2 media was added to each well. Plates were then irradiated with 20 J·cm^2 of red light (635 ± 10nm) using a Sorisa Photocare LED lamp source and returned to the incubator. 24h post irradiation, the MTT assay was performed to determine cell viability, as described above. The percentage of cell viability was calculated by normalizing absorbance values to that of corresponding untreated controls. To avoid attributing dark toxicity to phototoxicity, absorbance values were normalized to controls that had been treated with conjugate but had not been irradiated.

Results

ICAM-1 expression in microvascular EC is more upregulated by cytokine activation than by shear stress

HCAEC showed an 11-fold higher basal expression of ICAM-1 than HmVEC (Figure 1A). With respect to untreated controls, TNF-α stimulation upregulated HCAEC ICAM-1 expression by 4- fold, while HmVEC ICAM-1 expression increased about 20-fold (Figure 1A). All subsequent experiments were performed following TNF-α stimulation, to better recapitulate the inflammatory state of EC in pathologic angiogenesis (33,34). Untreated and TNF-α stimulated HmVEC and HCAEC were exposed to 0, 8 and 18 dyn/cm^2 to determine effects of shear stress on ICAM-1 expression. For TNF-α stimulated micro and macrovascular EC, exposure to 8 dyn/cm^2 did not significantly alter ICAM-1 expression compared to static conditions (Figure 1B, $P>0.05$). When exposed to 18 dyn/cm^2, ICAM-1 expression in HmVEC and HCAEC increased 2- fold and 5-fold, respectively (Figure 1B). For both static and 8 dyn/cm^2, ICAM-1 expression of HmVEC and HCAEC was not significantly different ($P>0.05$). Flow *per se* upregulated ICAM-1 expression in untreated HmVEC and HCAEC, but values were several orders of magnitude less than with cytokine stimulation (data not shown).

Influence of shear stress on the differential uptake of anti-ICAM-1 by HCAEC and HmVEC

Following TNF-α stimulation, both EC types showed similar anti-ICAM-1 uptake kinetics for the three shear stress levels studied (Figure 2). Under static (no flow) conditions, both EC displayed maximum antibody uptake at 4h of incubation ($P<0.05$) (Figure 2A). For 8 and 18 dyn/cm^2, maximum uptake shifted to 18 and 8 hours of incubation, respectively ($P<0.05$) (Figure 2B,C). For both EC types, the maximum uptake for 0 and 8 dyn/cm^2, at 4 and 18 hours respectively, did not significantly differ ($P>0.05$) (Figure 2A). The maximum at 18 dyn/cm^2 showed a 1.2-fold uptake increase for both EC types, with respect to the maximum uptakes at the lower shear stress levels (Figure 2C, $P<0.05$).

Synthesis and characterization of anti-ICAM-1-GlamTPPoEdaNCS

The novel porphycene GlamTPPoEdaNCS was characterized by ^{1}H and ^{13}C NMR spectra (Figure 3A, 3B). NMR spectra of the intermediates are shown in Supplemental Figures 1 and 2. The absorption spectrum of the anti-ICAM-1-porphycene exhibits three distinctive bands (Figure 3C). The absorption band with a maximum centered at 280 nm corresponds to the antibody , while absorption bands with maximums centered at 375nm and 655nm correspond to the porphycene characteristic Soret and Q bands, respectively (Figure 3C) (32,35). SDS-PAGE gel electrophoresis of the conjugate gave a predominant band at approximately 80 kDa MW as expected (data not shown).

ICAM-1 Targeting of HmVEC with anti-ICAM-porphycene depends upon TNF-α stimulation, while HCAEC does not

We assayed the ability of the new conjugate to efficiently target ICAM-1 receptor on EC and to provoke a triggered cellular response. Experiments involving the conjugate were conducted under static conditions only, given that previous experiments showed no significant difference between ICAM-1 expression and uptake of the antibody between static and 8 dyn/cm^2, which is the range of physiologic flow in tumor microvasculature.

To determine dark toxicity of the conjugate, untreated and TNF-α stimulated HCAEC and HmVEC were incubated with increasing concentrations of anti-ICAM-1-porphycene conjugate. In the range of concentrations studied (0.001-1.0μM), the conjugate caused dark toxicity only in TNF-α stimulated HCAEC, with an average viability of 74±22% with respect to non-irradiated controls (Figure 4A). Neither TNF-α stimulated HmVEC, nor unstimulated HmVEC and HCAEC, showed dark toxicity for any of the concentrations studied.

Phototoxic response was measured by incubating cells with a conjugate concentration of 1.0μM for 4h. The time of incubation, 4h, corresponds to the time of maximum uptake under static conditions, determined by the antibody uptake experiment described above(Figure 2A). Cultures were then irradiated with 635nm light at a power of 20J/cm^2 (Figure 4). Both untreated and cytokine-stimulated HCAEC exhibited phototoxic response, presenting 39±5.3% and 28±1.9% viability, respectively, with regard to non-irradiated controls (Figure 4B). In contrast, the conjugate was phototoxic to HmVEC only under TNF-α stimulation (Figure 4B). When irradiated, the viability of cytokine-stimulated HmVEC was significantly reduced to 32±3.7% ($P<0.05$), while untreated HmVEC did not show phototoxicity (113±22.3% viability in untreated HmVEC, calculated with respect to non-irradiated controls, Figure 4B).

Discussion

Photodynamic therapy (PDT) has become a well-established clinical treatment for cancer and other diseases (20,36). Here we propose a new therapeutic approach that combines PDT

with immunotargeting of microvascular endothelial cells (EC) to take advantage of cell-state and environmental cues of diseased tissue.

Years of research have led to the development of commercial PDT sensitizer agents that are currently being used in treatment with positive effects (20,36). The lack of sensitizer targeting, however, limits the effectiveness of PDT (19,20). High doses are required to counteract the lack of selectivity, leading to generalized photosensitivity of the patient and major difficulty in treating tumors found in sensitive regions such as the brain (20,36).

To enhance photosensitizer selectivity and delivery, previous studies have conjugated photosensitizers to monoclonal antibodies and antibody fragments (19,22). Traditional methods of conjugation, such as using activated esters or carbodiimide coupling of carboxy substituted photosensitizers, present problems related to antibody crosslinking or changes in the photophysics of the sensitizer (19,37). In the past decade, a highly effective method for sensitizer bioconjugation has been developed using mono-isothiocyanate porphyrins (19,20,23). Incorporating only one reactive thiocyanate (NCS) group in the molecular structure of porphyrin grants major advantages with respect to previous conjugation methods, two of which are: 1) no cross-linking occurs, given that only one amine-reactive NCS group exists in each porphyrin; 2) the generation of byproducts is prevented because the NCS group reacts spontaneously with amine groups of lysine residues by an addition reaction (19,20).

This is the first report that applies the isothiocyanate conjugation route to a porphycene molecule rather than a porphyrin. The specific porphycene selected for the study, GlamTPPo, presents a link in position 9, which enables functionalization in one site and allows the synthesis of an NCS-porphycene analogous to the mono-NCS porphyrins. This mono-NCS functionalization enabled the bioconjugation to anti-ICAM-1 to form a novel immunotargeted drug. Porphycenes present an important advantage over porphyrin molecules traditionally used in PDT. Porphyrins present a stronger absorption in the green light, which is readily absorbed by red blood cells (38), than the red light. During PDT, light must travel through a blood free field in order to activate the porphyrins accumulated at the site of interest. Thus, the use of porphyrins requires intravascular illumination, limiting this approach to use during invasive procedures or to treating superficial tumors or lesions (38). Conversely, the higher absorption of porphycenes in the red spectral region allows for the use of lasers as lower energy, noninvasive light sources that can easily penetrate tissue and activate sensitizers in greater depths (38-41).

The differential effects of the anti-ICAM-1-GlamTPPoNCS conjugate on macro and microvascular endothelial cells have major implications on the use of the conjugate as a PDT drug. In microvascular EC, the conjugate was only phototoxic to cytokine-activated cells. This finding suggests that the conjugate may be applicable as an exceptionally selective therapeutic agent capable of discriminating diseased (cytokine-activated) from healthy (untreated control) cells. In current PDT, accumulation of the sensitizer at the tumoral site relies solely on penetration into the newly formed and leaky neovasculature and retention due to the lack of sufficient lymphatic drainage (20). The ability of the novel conjugate to distinguish between cytokine-activated and healthy microvascular EC shows promise in enhancing drug delivery to the tumoral angiogenic neovasculature based on cell surface state.

The indiscriminate phototoxicity of the conjugate in healthy and stimulated HCAEC does not present a limitation for its potential use as a PDT agent. The localized nature of PDT relies on using an adequate light source that delivers light solely to the site of the tumor. Thus, though macrovascular EC showed similar phototoxicity regardless of cytokine

activation, the correct delivery of light should prevent illumination of healthy tissues and will avoid triggering phototoxicity to healthy macrovascular EC. Still, the dark toxicity observed in TNF-α stimulated HCAEC raises the question whether this novel drug would have toxic effects in tissues exhibiting inflammation at the time of therapy. If administered intravenously, like the widely used PDT drug Photofrin®, the novel conjugate might cause dark toxicity to macrovasculature. Local delivery may overcome this potential drawback with the added benefit of inducing vascular collapse provoked by the conjugate only in the vicinity of the tumor. Evaluating the conjugate in *in vivo* models will help elucidate what delivery method may be more suitable in a preclinical and clinical setting in order to minimize side effects on the macrovascular endothelial cells.

Targeting neovessels requires taking into account that the extracellular matrix below, the state of neighboring cells, and the hemodynamic environment above influence endothelium function. While differences in CAM expression with cytokine and shear stress exposure have been well explored as markers of endothelial cell inflammatory phenotype (42-44), the changes in anti-ICAM-1 uptake we observed open a new therapeutic window for endothelial targeting and treatment. Sensitizer efficacy may be increased by irradiating at the time of maximum uptake, which is conditioned by shear stress on the vasculature of the treated area. This would enable administering lower doses of sensitizer to the site of interest, helping to overcome generalized photosensitivity of patients.

One may consider as well applying such PDT drug conjugates to targeting angiogenic vessels in atherosclerotic plaques. As atheroma progresses, microvessels originating from adventitial vasa vasorum invade the plaque (28). The poorly formed EC-EC junctions of the premature neovessels are responsible for intraplaque hemorrhage, which contributes to the growth of atherosclerotic lesions, plaque destabilization and rupture (28,45). This notion has driven efforts in targeting neovessels to stabilize plaque, either by inhibiting plaque angiogenesis with anti-angiogenic factors or by pursuing vessel “maturation” through delivery of pro-angiogenic molecules (11,46-49). An attempt to treat atherosclerosis similarly to cancer, could involve targeting microvasculature with a PDT immunoconjugate. However, the mechanisms by which PDT causes tumor regression show little promise for treatment of atherosclerosis (50). Namely, efficacy of vascular targeted PDT in cancer relies on inducing vascular collapse(51), and in atherosclerosis this approach has the risk of intensifying intraplaque hemorrhage and plaque instability (28,46). Furthermore, PDT of cancer often causes post-illumination overexpression of proangiogenic factors such as vascular endothelial growth factor, cyclooxygenase-2 and matrix metalloproteases (52,53). Though anti-angiogenic factors can counteract this secondary effect in cancer, in an atherosclerotic plaque the high risk of accelerating the inflammatory response and the recruitment of monocytes makes this approach much less attractive. Further investigation is needed to assess if acting on the plaque microvasculature with the PDT conjugated drug described in this study, or other similar anti- CAM bioconjugates linked to molecules that promote plaque stabilization, could improve current treatments.

Immunotargeting of vascular endothelial cells has already been explored as a potentially powerful tool for correcting vascular function under diseased conditions (54). Extending this concept, our study presents a method of drug delivery to cell surface receptor ICAM-1 to a particular type of endothelial cells, namely microvascular endothelial cells. Shear stress and cytokine activation dictate CAM surface expression and modulate anti-ICAM binding differentially by macro and microvascular EC, which may be applied to treat pathologic neovascularization in certain diseases. We designed and synthesized a novel porphycene-anti- ICAM-1 compound which was able to distinguish between healthy and inflamed microvascular EC, inducing phototoxicity only in the latter. These findings contribute to the

recent search for targeted photodynamic sensitizers with potential to minimizing generalized sensitivity exploiting cell-surface interactions in a particular tissue or tissue state.

Supplementary Material

Refer to Web version on PubMed Central for supplementary material.

Acknowledgments

This work has been supported by the Spanish *Ministerio de Economía y Competitividad* through grants no. BFU2009-0984 and CTQ2010-20870-C03-01, as well as by the NIH grant NIH/NIGMS RO1/GM049039, Fundació Empreses IQS and POSIMAT. Part of the work was possible thanks to a MIT-Spain Seed Fund awarded to SN and MB. RRG thanks the Generalitat de Catalunya (DURSI) and Fons Social Europeu for a predoctoral fellowship. MCL thanks the Institut Químic de Sarrià (IQS) for a predoctoral fellowship.

References

1. Aird WC. Phenotypic heterogeneity of the endothelium: I. Structure, function, and mechanisms. Circulation [Internet]. 2007 Feb 2; 100(2):158–73. Available from: http://www.ncbi.nlm.nih.gov/pubmed/17272818.
2. Félétou, M. The Endothelium: Part 1: Multiple Functions of the Endothelial Cells—Focus on Endothelium-Derived Vasoactive Mediators. [Internet]. San Rafael (CA): Morgan & Claypool Life Sciences; 2011. Available from: http://www.ncbi.nlm.nih.gov/books/NBK57149/
3. Morigi BM, Zoja C, Figliuzzi M, Foppolo M, Micheletti G, Bontempelli M, et al. Fluid Shear Stress Modulates Surface Expression of Adhesion Molecules. Blood. 1995; 85(7):1696–703. [PubMed: 7535583]
4. Sheikh S, Rainger GE, Gale Z, Rahman M, Nash GB. Exposure to fluid shear stress modulates the ability of endothelial cells to recruit neutrophils in response to tumor necrosis factor-alpha: a basis for local variations in vascular sensitivity to inflammation. Blood [Internet]. 2003 Oct 15; 102(8): 2828–34. Available from: http://www.ncbi.nlm.nih.gov/pubmed/12829609.
5. Burke-Gaffney A, Hellewell PG. Tumour necrosis factor-alpha-induced ICAM-1 expression in human vascular endothelial and lung epithelial cells: modulation by tyrosine kinase inhibitors. British Journal of Pharmacology [Internet]. 1996 Nov; 119(6):1149–58. Available from: http://www.pubmedcentral.nih.gov/articlerender.fcgi?artid=1915891&tool=pmcentrez&rendertype=abstract.
6. Davies PF. Hemodynamic shear stress and the endothelum in cardiovascular pathophysiology. Nat Clin Pract Cardiovasc Med. 2010; 6(1):16–26. [PubMed: 19029993]
7. Sheski F, Natarajan V, Pottratz ST. Tumor necrosis factor-α stimulates attachment of small cell lung carcinoma to endothelial cells. Journal of Laboratory and Clinical Medicine. 1999; 133(3):265–73. [PubMed: 10072259]
8. Muzykantov VR, Atochina EN, Ischiropoulos H, Danilovt SM, Fisher AB. Immunotargeting of antioxidant enzymes to the pulmonary endothelium. PNAS. 1996; 93(May):5213–8. [PubMed: 8643555]
9. Kamizuru H, Kimura H, Yasukawa T, Tabata Y, Honda Y, Ogura Y. Monoclonal antibody-mediated drug targeting to choroidal neovascularization in the rat. Investigative Ophthalmology & Visual Science [Internet]. 2001 Oct; 42(11):2664–72. Available from: http://www.ncbi.nlm.nih.gov/pubmed/11581214.
10. Kozower BD, Christofidou-Solomidou M, Sweitzer TD, Muro S, Buerk DG, Solomides CC, et al. Immunotargeting of catalase to the pulmonary endothelium alleviates oxidative stress and reduces acute lung transplantation injury. Nature Biotechnology [Internet]. 2003 Apr; 21(4):392–8. Available from: http://www.ncbi.nlm.nih.gov/pubmed/12652312.
11. Winter PM, Neubauer AM, Caruthers SD, Harris TD, Robertson JD, Williams Ta, et al. Endothelial alpha(v)beta3 integrin-targeted fumagillin nanoparticles inhibit angiogenesis in atherosclerosis. Arteriosclerosis, Thrombosis, and Vascular Biology [Internet]. 2006 Sep; 26(9): 2103–9. Available from: http://www.ncbi.nlm.nih.gov/pubmed/16825592.

12. Wu H, Li P. Proteins Expressed on Tumor Endothelial Cells as Potential Targets for Anti-Angiogenic Therapy. Journal of Cancer Molecules. 2008; 4(1):17–22.
13. Bhowmick, T.; Berk, E.; Cui, X.; Muzykantov, VR.; Muro, S. Journal of Controlled Release [Internet]. Vol. 157. Elsevier B.V; 2012 Feb 10. Effect of flow on endothelial endocytosis of nanocarriers targeted to ICAM-1; p. 485-92.Available from: http://www.ncbi.nlm.nih.gov/pubmed/21951807 [2013 Jan 17]
14. Ding B, Dziublam T, Shuvaev V, Muro S, Muzykantov V. Advanced drug delivery systems that target the vascular endothelium. Molecular Interventions. 2006; 6(2):98–112. [PubMed: 16565472]
15. Muro S, Dziubla T, Qiu W, Leferovich J, Cui X, Berk E, et al. Endothelial Targeting of High-Affinity Multivalent Polymer Nanocarriers Directed to Intercellular Adhesion Molecule 1. J of Pharmacology and Experimental Therapeutics. 2006; 317(3):1161–9.
16. Rothlein R, Dustin ML, Marlin SD, Springer Ta. A human intercellular adhesion molecule (ICAM-1) distinct from LFA-1. Journal of Immunology [Internet]. 1986 Aug 15; 137(4):1270–4. Available from: http://www.ncbi.nlm.nih.gov/pubmed/3525675.
17. Pober, J. Effects of tumour necrosis factor and related cytokines on vascular endothelial cells. Ciba Foundation Symposium; 1987. p. 170-84.
18. Muro S, Gajewski C, Koval M, Muzykantov VR. ICAM-1 recycling in endothelial cells: a novel pathway for sustained intracellular delivery and prolonged effects of drugs. Blood [Internet]. 2005 Jan 15; 105(2):650–8. Available from: http://www.ncbi.nlm.nih.gov/pubmed/15367437.
19. Staneloudi C, Smith Ka, Hudson R, Malatesti N, Savoie H, Boyle RW, et al. Development and characterization of novel photosensitizer : scFv conjugates for use in photodynamic therapy of cancer. Immunology [Internet]. 2007 Apr; 120(4):512–7. Available from: http://www.pubmedcentral.nih.gov/articlerender.fcgi?artid=2265903&tool=pmcentrez&rendertype=abstract.
20. Smith K, Malatesti N, Cauchon N, Hunting D, Lecomte R, Van Lier JE, et al. Mono- and tri-cationic porphyrin-monoclonal antibody conjugates: photodynamic activity and mechanism of action. Immunology [Internet]. 2011 Feb; 132(2):256–65. Available from: http://www.pubmedcentral.nih.gov/articlerender.fcgi?artid=3045661&tool=pmcentrez&rendertype=abstract.
21. Ragàs X, Sánchez-García D, Ruiz-González R, Dai T, Agut M, Hamblin MR, et al. Cationic porphycenes as potential photosensitizers for antimicrobial photodynamic therapy. Journal of Medicinal Chemistry [Internet]. 2010 Nov 11; 53(21):7796–803. Available from: http://www.pubmedcentral.nih.gov/articlerender.fcgi?artid=2981434&tool=pmcentrez&rendertype=abstract.
22. Clarke OJ, Boyle RW. Isothiocyanatoporphyrins, useful intermediates for the conjugation of porphyrins with biomolecules and solid supports. Chemical Communications. 1999; (21):2231–2.
23. Hudson R, Carcenac M, Smith K, Madden L, Clarke OJ, Pèlegrin A, et al. The development and characterisation of porphyrin isothiocyanate-monoclonal antibody conjugates for photoimmunotherapy. British Journal of Cancer [Internet]. 2005 Apr 25; 92(8):1442–9. Available from: http://www.pubmedcentral.nih.gov/articlerender.fcgi?artid=2362018&tool=pmcentrez&rendertype=abstract.
24. Carmeliet P. Angiogenesis in health and disease. Nature Medicine [Internet]. 2003 Jun; 9(6):653–60. Available from: http://www.ncbi.nlm.nih.gov/pubmed/12778163.
25. Roberts WG, Palade GE, Palade E. Neovasculature Induced by Vascular Endothelial Growth Factor Is Fenestrated Neovasculature Induced by Vascular Endothelial Growth Factor Is Fenestrated. Cancer Research. 1997; 57:765–72. [PubMed: 9044858]
26. Griffioen, aW; Molema, G. Angiogenesis: potentials for pharmacologic intervention in the treatment of cancer, cardiovascular diseases, and chronic inflammation. Pharmacological reviews [Internet]. 2000 Jun; 52(2):237–68. Available from: http://www.ncbi.nlm.nih.gov/pubmed/10835101.
27. Winter PM, Neubauer AM, Caruthers SD, Harris TD, Robertson JD, Williams Ta, et al. Endothelial alpha(v)beta3 integrin-targeted fumagillin nanoparticles inhibit angiogenesis in atherosclerosis. Arteriosclerosis, Thrombosis, and Vascular Biology [Internet]. 2006 Sep; 26(9):2103–9. Available from: http://www.ncbi.nlm.nih.gov/pubmed/16825592.

28. Moreno PR, Purushothaman K-R, Sirol M, Levy AP, Fuster V. Neovascularization in human atherosclerosis. Circulation [Internet]. 2006 May 9; 113(18):2245–52. Available from: http://www.ncbi.nlm.nih.gov/pubmed/16684874.
29. Yasukawa T, Hoffmann S, Eichler W, Friedrichs U, Wang Y, Wiedemann P. Inhibition of experimental choroidal neovascularization in rats by an alpha(v)-integrin antagonist. Current Eye Research. 2004; 28(5):359–66. [PubMed: 15287373]
30. Danhier, F.; Vroman, B.; Lecouturier, N.; Crokart, N.; Pourcelle, V.; Freichels, H., et al. Journal of Controlled Release [Internet]. Vol. 140. Elsevier B.V.; 2009 Dec 3. Targeting of tumor endothelium by RGD-grafted PLGA-nanoparticles loaded with paclitaxel; p. 166-73.Available from: http://www.ncbi.nlm.nih.gov/pubmed/19699245 [2012 Nov 13]
31. Balcells M, Fernández Suárez M, Vázquez M, Edelman ER. Cells in fluidic environments are sensitive to flow frequency. Journal of Cellular Physiology [Internet]. 2005 Jul; 204(1):329–35. Available from: http://www.ncbi.nlm.nih.gov/pubmed/15700266.
32. Carcenac M, Larroque C, Langlois R, Van Lier JE, Artus JC, Pèlegrin a. Preparation, phototoxicity and biodistribution studies of anti-carcinoembryonic antigen monoclonal antibody-phthalocyanine conjugates. Photochemistry and photobiology [Internet]. 1999 Dec; 70(6):930–6. Available from: http://www.ncbi.nlm.nih.gov/pubmed/10628305.
33. Hayden MR, Tyagi SC. Vasa vasorum in plaque angiogenesis, metabolic syndrome, type 2 diabetes mellitus, and atherosclerosis: a malignant transformation. Cardiovascular Diabetology. 2004; 16(1575):1–16. [PubMed: 14761253]
34. Sainson RC, Johnston Da, Chu HC, Holderfield MT, Nakatsu MN, Crampton SP, et al. TNF primes endothelial cells for angiogenic sprouting by inducing a tip cell phenotype. Blood [Internet]. 2008 May 15; 111(10):4997–5007. Available from: http://www.pubmedcentral.nih.gov/articlerender.fcgi?artid=2384130&tool=pmcentrez&rendertype=abstract.
35. Lan Z, Nonell S, Barbatti M. Theoretical Characterization of Absorption and Emission Spectra of an Asymmetric Porphycene. Journal of Physical Chemistry A. 2012; 116(13):3366–76.
36. Agostinis P, Berg K, Cengel KA, Foster TH, Girotti AW, Gollnick SO, et al. Photodynamic Therapy of Cancer: An Update. CA Cancer J Clin. 2011; 61:250–81. [PubMed: 21617154]
37. Vrouenraets MB, Visser GW, Stewart Fa, Stigter M, Oppelaar H, Postmus PE, et al. Development of meta-tetrahydroxyphenylchlorin-monoclonal antibody conjugates for photoimmunotherapy. Cancer Research [Internet]. 1999 Apr 1; 59(7):1505–13. Available from: http://www.ncbi.nlm.nih.gov/pubmed/10197621.
38. Waksman R, McEwan P, Moore T, Pakala R, Kolodgie F, Hellinga D, et al. PhotoPoint photodynamic therapy promotes stabilization of atherosclerotic plaques and inhibits plaque progression. Journal of the American College of Cardiology. 2008; 52(12):1024–32. [PubMed: 18786486]
39. Stockert JC, Canete M, Juarranz A, Villanueva A, Horobin RW, Borrell JI, et al. Porphycenes: Facts and Prospects in Photodynamic Therapy of Cancer. Current Medicinal Chemistry. 2007; 14(9):997–1026. [PubMed: 17439399]
40. Gawinkowski S, Orzanowska G, Izdebska K, Senge MO, Waluk J. Bridging the gap between porphyrins and porphycenes: substituent-position-sensitive tautomerism and photophysics in meso-diphenyloctaethylporphyrins. Chemistry (Weinheim an der Bergstrasse, Germany) [Internet]. 2011 Aug 29; 17(36):10039–49. Available from: http://www.ncbi.nlm.nih.gov/pubmed/21796691.
41. Rubio N, Prat F, Bou N, Borrell JI, Teixidó J, Villanueva Á, et al. A comparison between the photophysical and photosensitising properties of tetraphenyl porphycenes and porphyrins. New J of Chem. 2005; 29:378–84.
42. Packard RRS, Libby P. Inflammation in atherosclerosis: from vascular biology to biomarker discovery and risk prediction. Clinical Chemistry [Internet]. 2008 Jan; 54(1):24–38. Available from: http://www.ncbi.nlm.nih.gov/pubmed/18160725.
43. Methe H, Balcells M, Alegret MDC, Santacana M, Molins B, Hamik A, et al. Vascular bed origin dictates flow pattern regulation of endothelial adhesion molecule expression. American Journal of Physiology [Internet]. 2007 May; 292(5):H2167–75. Available from: http://www.ncbi.nlm.nih.gov/pubmed/17209004.

44. Luscinskas FW, Gimbrone Ma. Endothelial-dependent mechanisms in chronic inflammatory leukocyte recruitment. Annual Review of Medicine [Internet]. 1996 Jan.47:413–21. Available from: http://www.ncbi.nlm.nih.gov/pubmed/8712792.
45. Virmani R, Kolodgie FD, Burke AP, Finn AV, Gold HK, Tulenko TN, et al. Atherosclerotic plaque progression and vulnerability to rupture: angiogenesis as a source of intraplaque hemorrhage. Arteriosclerosis, thrombosis, and vascular biology [Internet]. 2005 Oct; 25(10):2054–61. Available from: http://www.ncbi.nlm.nih.gov/pubmed/16037567.
46. Doyle B, Caplice N. Plaque neovascularization and antiangiogenic therapy for atherosclerosis. Journal of the American College of Cardiology [Internet]. 2007 May 29; 49(21):2073–80. Available from: http://www.ncbi.nlm.nih.gov/pubmed/17531655.
47. Vuorio T, Jauhiainen S, Ylä-Herttuala S. Pro- and anti-angiogenic therapy and atherosclerosis with special emphasis on vascular endothelial growth factors. Expert Opin Biol Therapy [Internet]. 2012 Jan; 12(1):79–92. Available from: http://www.ncbi.nlm.nih.gov/pubmed/22115316.
48. Slevin M, Krupinski J, Badimon L. Controlling the angiogenic switch in developing atherosclerotic plaques: possible targets for therapeutic intervention. Journal of Angiogenesis Research [Internet]. 2009 Jan.1(Cvd):4. Available from: http://www.pubmedcentral.nih.gov/articlerender.fcgi?artid=2776234&tool=pmcentrez&rendertype=abstract.
49. Moulton KS, Vakili K, Zurakowski D, Soliman M, Butterfield C, Sylvin E, et al. Inhibition of plaque neovascularization reduces macrophage accumulation and progression of advanced atherosclerosis. PNAS [Internet]. 2003 Apr 15; 100(8):4736–41. Available from: http://www.pubmedcentral.nih.gov/articlerender.fcgi?artid=153625&tool=pmcentrez&rendertype=abstract.
50. Muller JE. New light on an old problem photodynamic therapy for atherosclerosis. Journal of the American College of Cardiology [Internet]. 2008 Sep 16; 52(12):1033–4. Available from: http://www.ncbi.nlm.nih.gov/pubmed/18786487.
51. Olivo M, Bhuvaneswari R, Lucky SS, Dendukuri N, Soo-Ping Thong P. Targeted Therapy of Cancer Using Photodynamic Therapy in Combination with Multi-faceted Anti-Tumor Modalities. Pharmaceuticals [Internet]. 2010 May 14; 3(5):1507–29. Available from: http://www.mdpi.com/1424-8247/3/5/1507/.
52. Bhuvaneswari R, Gan YY, Soo KC, Olivo M. The effect of photodynamic therapy on tumor angiogenesis. Cellular and molecular life sciences : CMLS [Internet]. 2009 Jul; 66(14):2275–83. Available from: http://www.ncbi.nlm.nih.gov/pubmed/1933355.
53. He, C.; Fateye, B.; Chen, B. Kessel, DH., editor. [2013 Mar 15] Combination of vascular targeting PDT with combretastatin A4 phosphate; Photodynamic Therapy: Back to the Future [Internet]. 2009. p. 738032-738032-6.Available from: http://proceedings.spiedigitallibrary.org/proceeding.aspx?articleid=782589
54. Spragg DD, Alford DR, Greferath R, Larsen CE, Lee KD, Gurtner GC, et al. Immunotargeting of liposomes to activated vascular endothelial cells: a strategy for site-selective delivery in the cardiovascular system. PNAS [Internet]. 1997 Aug 5; 94(16):8795–800. Available from: http://www.pubmedcentral.nih.gov/articlerender.fcgi?artid=23135&tool=pmcentrez&rendertype=abstract.

Abbreviations

EC	Endothelial cells
CAM	Cellular adhesion molecule
GlamTPPo	glutaramide-2,7,12,17-tetra-phenylporphycene
HCAEC	Human coronary artery endothelial cells
HmVEC	Human microvascular endothelial cells
ICAM-1	Intercellular adhesive molecule 1

(A)

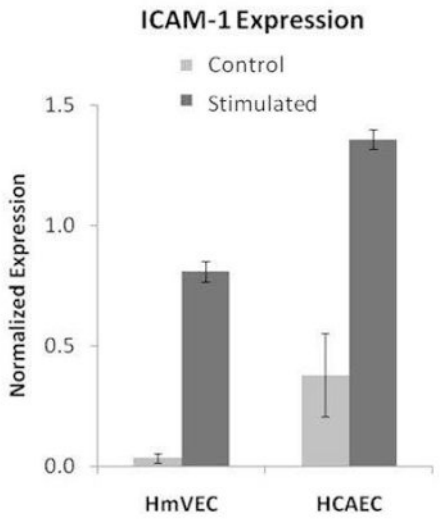

(B)

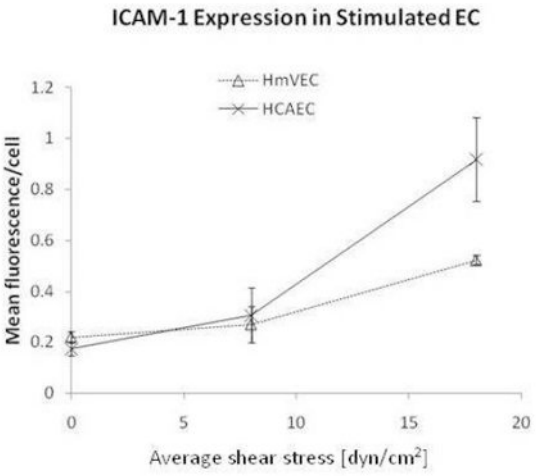

(C)

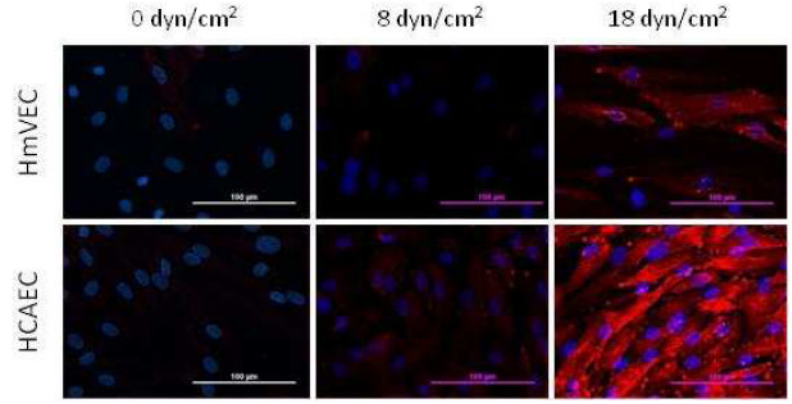

Figure 1.

Effects of cytokine stimulation and shear stress on ICAM-1 expression in HCAEC and HmVEC: (A) Western blot results normalized to tubulin show differential ICAM-1 basal levels and upregulation in macro and microvascular EC exposed to cytokine-induced inflammation (±TNF- α). (B) Immunostaining of HCAEC and HmVEC, which were seeded in parallel plate flow chambers, stimulated with TNF-α and exposed to 0, 8 or 18 dyn/cm^2, revealed upregulation of ICAM-1 expression with increasing shear stress for both endothelial cell types. (C) Fluorescent images of HmVEC and HCAEC exposed to 0, 8 and 18 dyn/cm^2, used for the ICAM-1 expression quantification shown in Panel B.

(A)

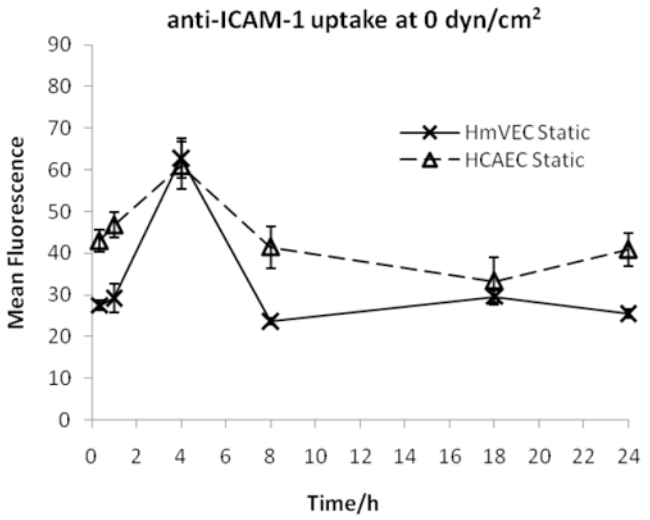

(B)

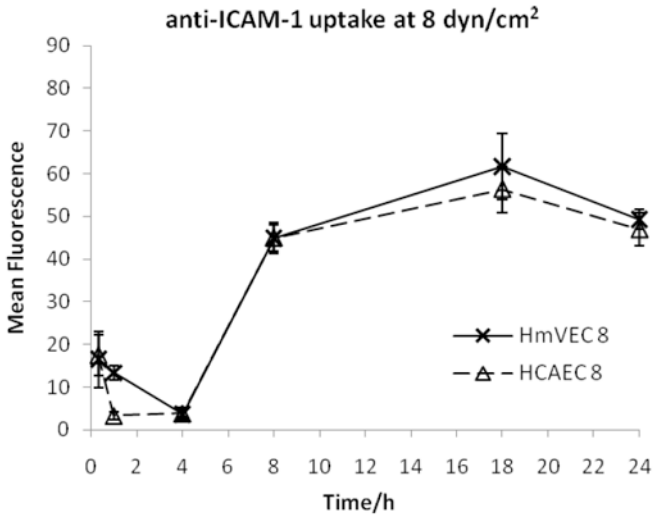

(C)

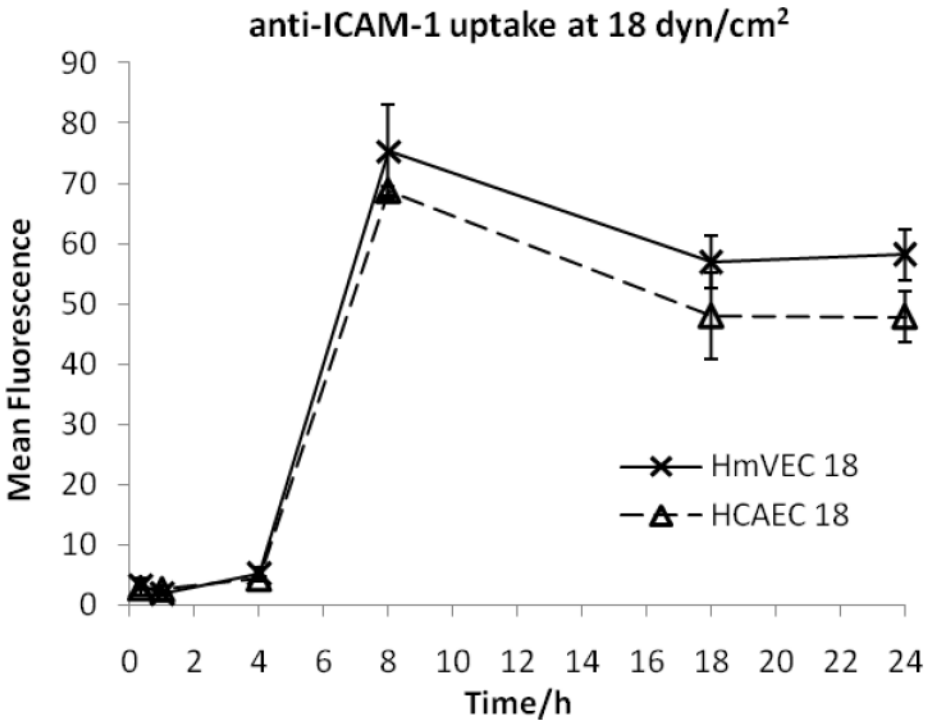

Figure 2.

Microvascular EC (HmVEC) and macrovascular EC (HCAEC) were seeded in parallel plate flow chambers and stimulated with TNF-α. Chambers were perfused with media containing FITCanti- ICAM-1, exerting shear stress levels of 0, 8 or 18 dyn/cm^2 on cells. The anti-ICAM-1 uptake kinetics for (A) 0 dyn/cm^2, (B) 8 dyn/cm^2 and (C) 18 dyn/cm^2 were obtained by quantification of fluorescent images taken at time points from 30min to 24h.

(A)

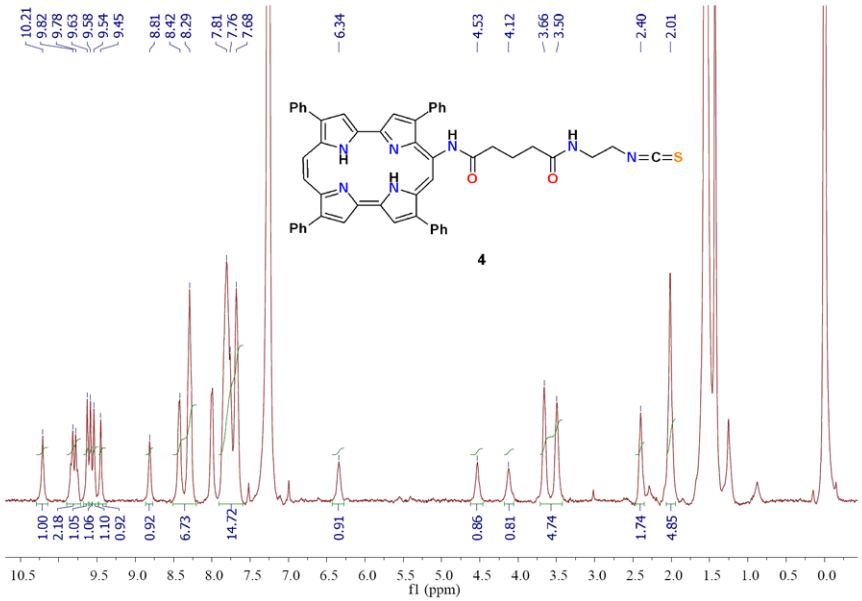

(B)

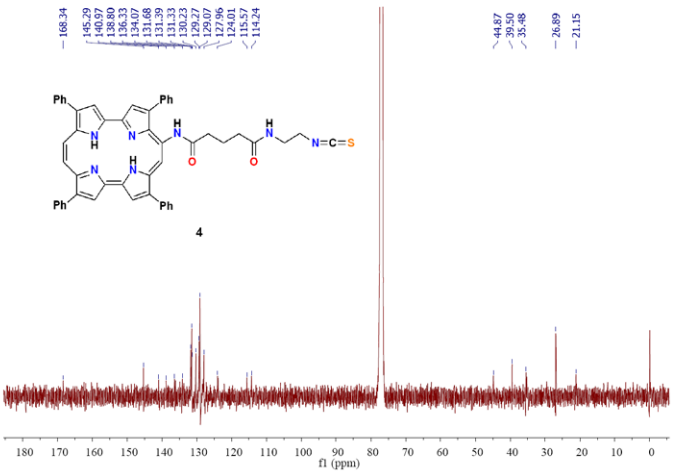

(C)

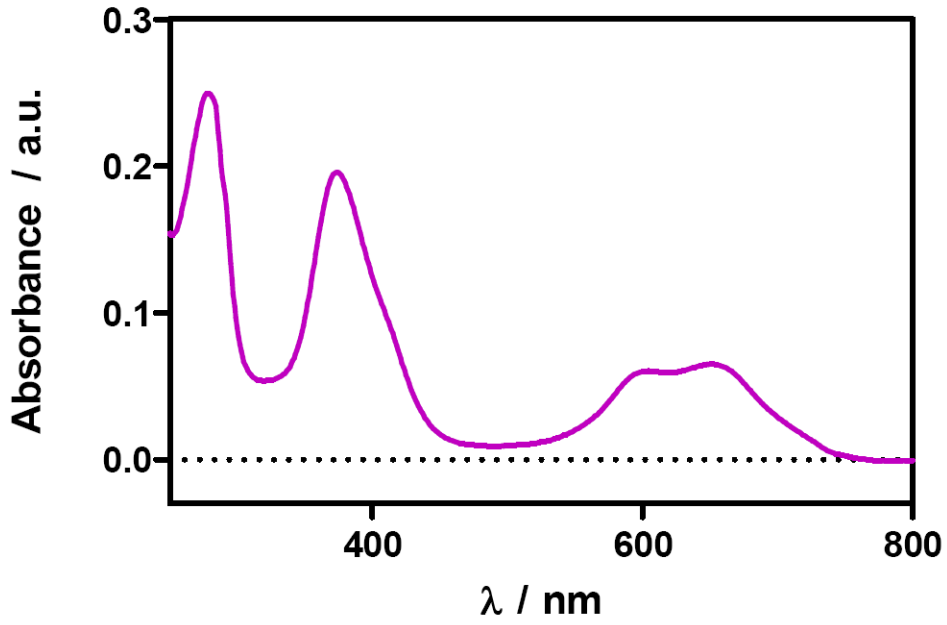

Figure 3.

Characterization of EdaGlamNCSTPPo and anti-ICAM-1 conjugate.

A) ^{1}H-RMN of EdaGlamNCSTPPo ($CDCl_3$):

^{1}H NMR (400 MHz, $CDCl_3$) δ 10.21 (s, 1H), 9.82 (d, 1H), 9.78 (d, 1H), 9.63 (s, 1H), 9.58 (s, 1H), 9.54 (s, 1H), 9.45 (s, 1H), 8.81 (s, 1H), 8.44 – 8.29 (m, 7H), 7.91 – 7.60 (m, 15H), 6.34 (s, 1H), 4.53 (s, 1H), 4.12 (s, 1H), 3.58 (m, 4H), 2.40 (s, 2H), 2.01(m,5H)

B) ^{13}C-RMN of EdaGlamNCSTPPo (CDCl3):

^{13}C NMR (100 MHz, $CDCl_3$): δ $CDCl_3$ (ppm): δ168.34 (C=O am), 145.29, 140.97, 138.80, 136.33, 134.07, 131.68, 131.39, 131.33, 130.23, 129.27, 129.07, 127.96, 124.01, 115.57, 114.24, 44.87 (CH_2), 39.50 (CH_2), 35.48 (CH_2), 26.89 (CH_2), 21.15 (CH_2).

HRMS (ESI-TOF): m/z calculated for C52H41 N7O2S 827,3042 ; found 827,3095.

C) The UV-Vis absorbance spectrum of the conjugate shows three characteristic absorption bands used to characterize the conjugate. The protein absorption band is found at 280 nm, while the two characteristics bands of the porphycene, the Soret and Q bands, are centered at 375 nm and 655 nm, respectively.

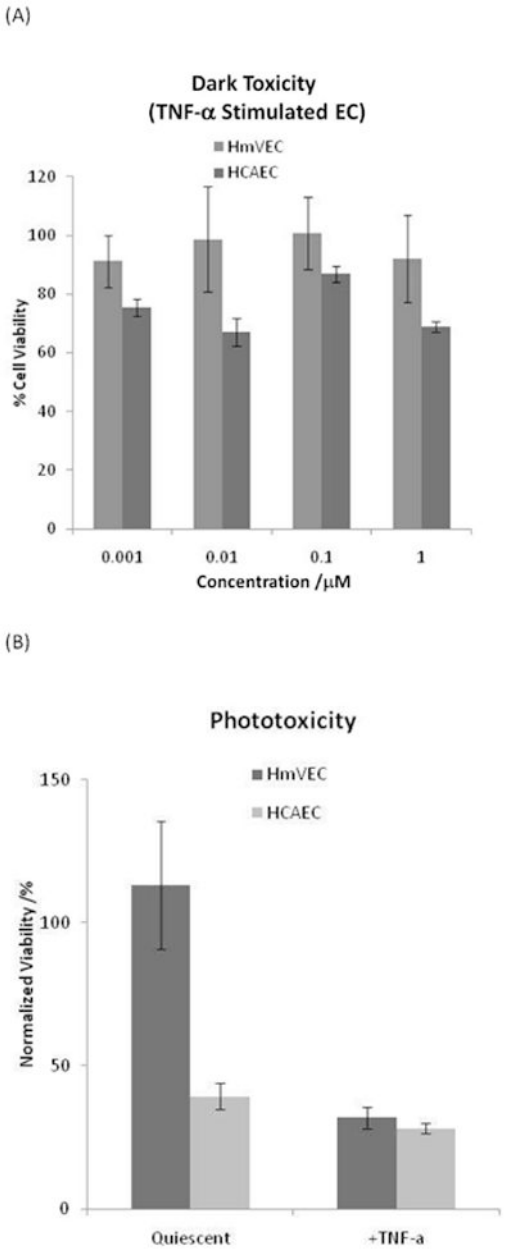

Figure 4.

Dark toxicity and phototoxicity of the anti-ICAM-1-porphycene conjugate were evaluated for HmVEC and HCAEC. (A) The immunoconjugate caused dark toxicity in TNF-α stimulated HCAEC but not in TNF-α stimulated HmVEC. Unstimulated controls incubated with the same conjugate concentrations did not present phototoxicity (results not shown). (B) Differential phototoxic effects were observed with varying endothelial phenotype. For microvascular EC, the conjugate was phototoxic to TNF-α stimulated, but not untreated, HmVEC. Conversely, the conjugate was phototoxic to HCAEC regardless of TNF-α stimulation.

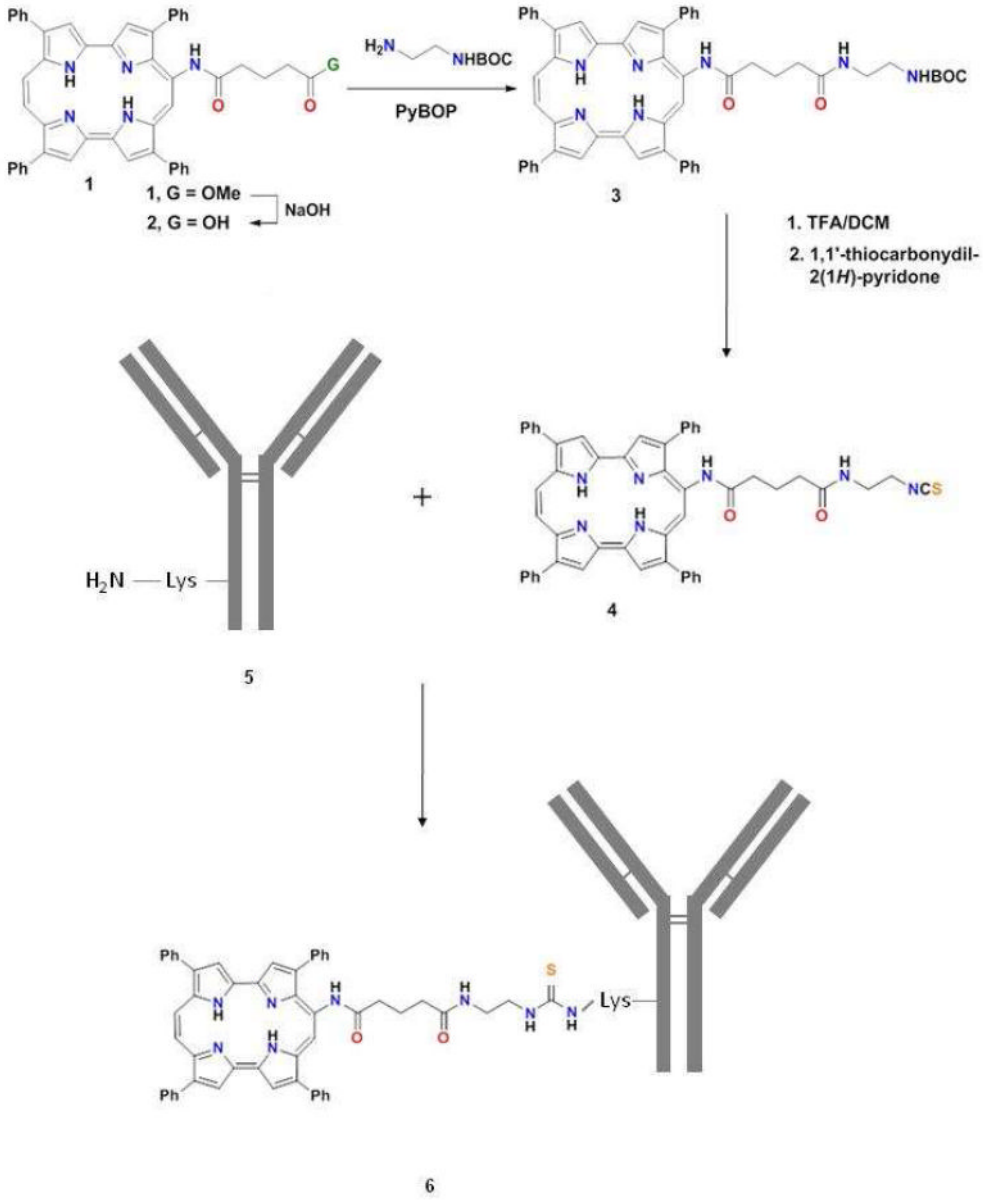

Scheme 1.

The precursor porphycene GlamTPPo (1) was functionalized with an isothiocyanate group to give EdaGlamNCSTPPo (4). This porphycene was conjugated to the ICAM-1 antibody (5) through thiourea bonds, resulting from the reaction between isothiocyanate group with the amines of anti-ICAM-1 lysine residues (6).